Journal of Power Sources 197 (2012) 102–106

Contents lists available at SciVerse ScienceDirect

Journal of Power Sources

journal homepage: www.elsevier.com/locate/jpowsour

Short communication

Fuel cell electrode structures containing sulfonated organosilane-based proton conductors

Jennie I. Eastcott, Kaitlyn M. Yarrow, Andrew W. Pedersen, E. Bradley Easton*

Faculty of Science, University of Ontario Institute of Technology, 2000 Simcoe Street North, Oshawa, Ontario, Canada L1H 7K4

ARTICLE INFO

Article history:
Received 13 July 2011
Received in revised form 31 August 2011
Accepted 9 September 2011
Available online 16 September 2011

Keywords:
Ceramic carbon electrodes
PEM fuel cell
Sol–gel
Proton conductivity

ABSTRACT

Ceramic carbon electrodes (CCE) for PEM fuel cells have been prepared in a one-pot procedure from a mixture of tetra ethyl orthosilicate (TEOS) and 3-trihydroxysilyl-1-propanesulfonic acid (TPS) polymerized in the presence of a platinized carbon with concurrent spray deposition of the partially gelled ink onto a gas diffusion layer. The CCE showed fuel cell performance comparable to commercially available Nafion-based cathodes. This high activity is explained in terms of the high electrochemically active surface area resulting from the enhanced proton conductivity in the CCE.

1. Introduction

Proton exchange membrane fuel cells continue to be seen as an important energy technology with minimal environmental impact. However, the technology still faces several challenges that must be addressed before it can be considered economically viable for large scale implementation. Currently, Pt is the best performing cathode catalyst but it is an expensive and somewhat rare metal. Thus, modern research aims to reduce the amount of catalyst required by improving the utilization of Pt surface area.

Catalyst layers are normally composed of a carbon-supported Pt catalyst that has been mixed with Nafion ionomer [1]. Nafion serves to increase proton conductivity within the catalyst layer, which improves catalyst utilization [2]. However, excess Nafion is detrimental to fuel cell performance since it restricts gas flow (and is also expensive). Consequently, there is a great desire to reduce or replace Nafion with a cheaper and more effective material. Two main approaches have been reported in literature to achieve this. The first approach has been to reduce the amount of Nafion by adding other proton conducting materials to the catalyst layer. Most commonly, this has been done through surface modification of the carbon support [3–10]. The second approach has been to entirely replace Nafion in the catalyst layer with a hydrocarbon-based ionomer, which has been recently reviewed by Peron and co-workers [11]. Common hydrocarbon ionomers studied include sulfonated poly(ether ether ketone) (SPEEK) [12–16], sulfonated polyphosphazene [17], and polysulfones [18].

One emerging type of electrode structure is a ceramic carbon electrode (CCE). CCEs consist of electronically conductive carbon particles that are bound together by a ceramic binder formed through the sol–gel process [19,20] and are promising candidates for electrochemical applications, including fuel cells [21–23]. We have developed a CCE fabrication procedure where the organosilane precursors are mixed with the (catalyzed or un-catalyzed) carbon in monomer form, and subsequently polymerized and have demonstrated the viability of SiO_2-based CCEs for H_2/O_2 fuel cells electrodes [22]. While Nafion-based electrodes outperformed the SiO_2-based CCE, the conductivity and ECSA for these layers were impressive considering there were no highly acidic proton-conducting functional groups.

Here we report 3-trihydroxysilyl-1-propanesulfonic acid/TEOS-based CCE's prepared by in situ polymerization of the silane with concurrent spray deposition of the partially gelled ink. The fuel cell performance of these CCEs are reported and related to proton conductivity within the catalyst layer.

2. Experimental

2.1. CCE fabrication

The CCE material was prepared using a base-catalyzed procedure reported in detail elsewhere [22]. Briefly, 20% Pt on Vulcan XC72 carbon black (E-TEK BASF, 18.2 wt% Pt as confirmed by TGA) was dispersed in a solution of deionized water and methanol.

* Corresponding author. Tel.: +1 905 721 8668x2936; fax: +1 905 721 3304.
E-mail address: Brad.Easton@uoit.ca (E.B. Easton).

0378-7753/$ – see front matter © 2011 Elsevier B.V. All rights reserved.
doi:10.1016/j.jpowsour.2011.09.023

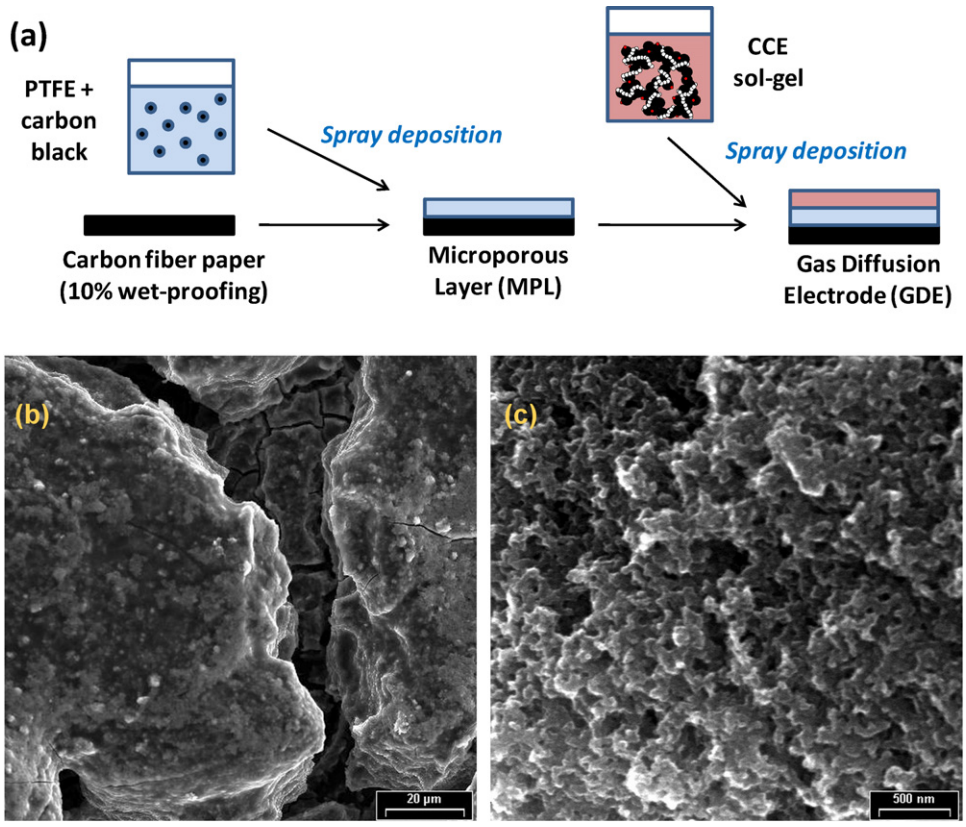

Fig. 1. (a) Schematic illustration of the synthesis and concurrent deposition of the SS-CCE catalyst layer to form fuel cell electrodes. SEM images obtained for CCE-based catalyst layers at (b) lower and (c) higher magnification.

To this, TPS (Gelest) and TEOS (Sigma) were added drop-wise in a 5:95 TPS-to-TEOS mole ratio. The mixture was allowed to gel for ca. 72 h after which the partially gelled mixture was spray applied onto a gas diffusion layer (GDL) using an air brush. The GDL used was prepared in-house using the procedure reported by Qi and Kaufman [24] and consisted of CFP (Toray TPGH-090, 10 wt% wet-proofing) coated with a Vulcan XC72/Teflon microporous layer (MPL, 2 mg cm^{-2} Vulcan carbon, 39 wt% Teflon). A schematic diagram of CCE preparation process is shown in Fig. 1(a). After deposition, the resulting electrode was dried for 30 min at both room temperature and 135 °C. The resulting electrode had a Pt loading of 0.34 mg cm^{-2} and a total silicate loading of 40 wt% and is hereafter referred to as SS-CCE.

2.2. Materials characterization

Thermogravimetric analysis (TGA) was performed using a TA Instruments Q600 SDT thermal analyzer. Samples were heated from room temperature up to 800 °C at a rate of 20 °C min^{-1} under flowing air (50 mL min^{-1}). BET surface areas were measured using a Gemini VII 2390 Series surface area analyzer. Scanning electron microscopy (SEM) images of the CCE layer were acquired using a JOEL JSM 6400 SEM.

2.3. Electrochemical measurements

Fuel cell membrane and electrode assemblies (MEA) were prepared by hot-pressing (150 kg cm^{-2} for 90 s at 130 °C) a 5-cm^2 test electrode (cathode) and a similar sized commercial anode (ELAT A6STDSIV2.1 Pt loading = 0.50 mg cm^{-2}, proprietary ionomer loading) across a Nafion NRE212 membrane. For comparison, a MEA was prepared using an ELAT electrode as both the test electrode and the anode. MEAs were tested in a 5-cm^2 fuel cell test fixture (Fuel Cell Technologies). Fuel cell testing was performed at a cell temperature of 80 °C, with feed gases (H_2 and O_2) humidified at 80 °C and pressurized to 10 psig (170 kPa) at the outlets.

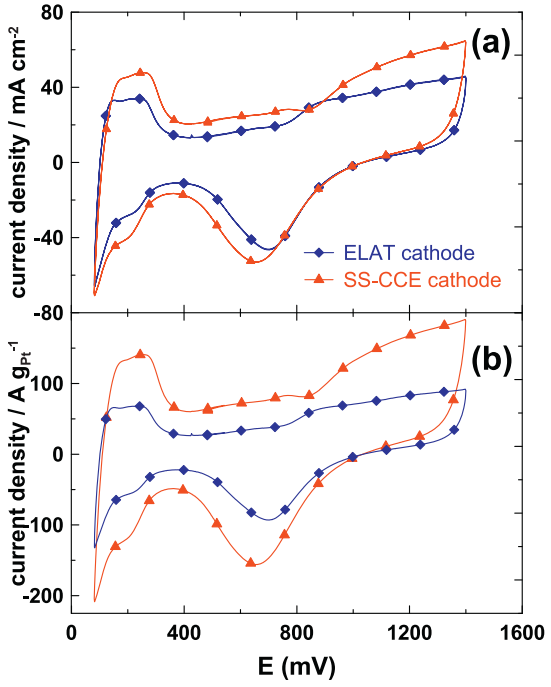

Fig. 2. Comparison of the CVs obtained for the SS-CCE cathode catalyst layer with that obtained with a Nafion-based ELAT cathode catalyst layer: (a) as acquired and (b) normalized to the Pt loading in each electrode. Measurements were made at 30 °C with an N_2-purged cathode compartment at 100% RH.

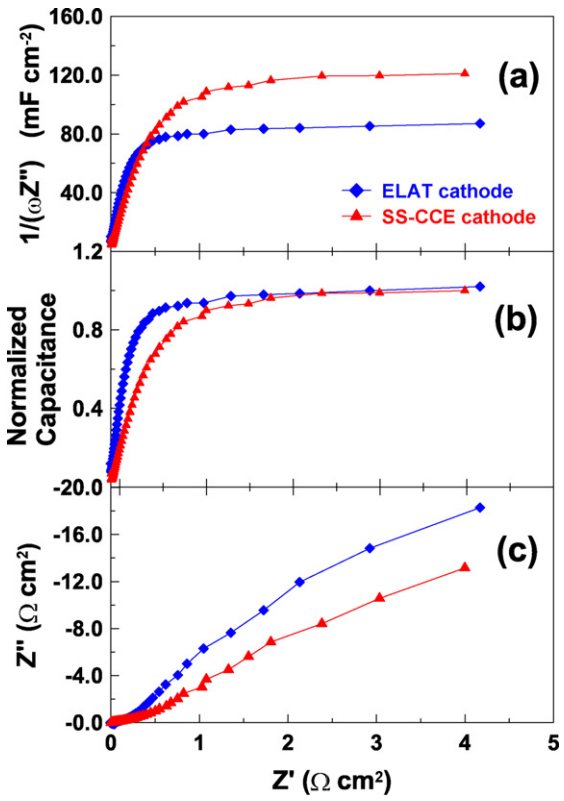

Fig. 3. Comparison of the EIS responses obtained for the SS-CCE cathode catalyst layer with that obtained with a Nafion-based ELAT cathode catalyst layer plotted as (a) capacitance plots and (b) normalized capacitance plots and (c) Nyquist plots. Measurements were made at 30 °C with an N_2-purged cathode compartment at 100% RH.

All cyclic voltammetry (CV) and electrochemical impedance spectroscopy (EIS) measurements were performed at 30 °C with humidified N_2 at the cathode and with the H_2 electrode serving as both the reference and the counter electrode. Measurements were performed using a Solartron 1470E Multichannel Potentiostat and a 1260 frequency response analyzer controlled using Multistat software (Scribner Associates). Impedance spectra were collected over a frequency range of 100 kHz to 0.1 Hz at a DC bias potential of 0.425 V.

3. Results

3.1. Materials characterization

The Pt and silicate loading for the SS-CCE cathode was confirmed by performing TGA under air. Under these conditions, the decomposition of the sulfonic acid group, the combustion of the organic side chain and the carbon black can be resolved, allowing the determination of the wt% of the each component [22,25,26]. TGA indicated that the CCE had an overall silicate content of 40 wt%, of which 6 mol% was TPS (balance TEOS), and 60 wt% platinized carbon. The compositions for all electrode samples are listed in Table 1.

In our previous work the CCE was allowed completely gel into a monolith, after which it was dried, ground into a fine powder, suspended in solution, and sprayed onto the GDL. In this work we have been able to spray deposit the partially gelled SS-CCE material directly onto the GDL. The presence of a MPL between the catalysts layer and carbon fibre paper (CFP) was determined to be essential for strong adhesion. SEM images for SS-CCE catalyst layer are shown in Fig. 1(b) and (c) which shows that homogeneous layers with a high degree of micro/meso-porosity were produced. BET analysis indicates that the SS-CCE catalyst layer has a surface area of 382 $m^2\ g^{-1}$, substantially larger than that of the bare Vulcan carbon (250 $m^2\ g^{-1}$) but smaller than the pure TEOS sample (514 $m^2\ g^{-1}$). The reduction in BET surface area upon addition of TPS is likely due to the presence of the organic side chain, which reduces the free volume within the structure.

3.2. Electrochemical characterization

Fig. 2 compares the CVs obtained for the SS-CCE to that obtained for the ELAT electrode. The area under the H_{ads} peaks in Fig. 2(a) was used to determine the electrochemical surface area (ECSA) of each, which are listed Table 1. Large, well-defined peaks were obtained for the SS-CCE cathode which are similar in shape to that obtained with the Nafion-based ELAT electrode and are much more well-defined (and larger) that those obtained for our previous SiO_2-based CCE's [22], indicating that the addition of a small amount of TPS to the SiO_2 network (6 mol%) has a drastic impact on ECSA. Since both electrodes were prepared from E-Tek 20% Pt on Vulcan XC72 carbon black, which is known to have an average Pt particle diameter of ca. 3 nm [27,28], Pt utilization can also be calculated. The SS-CCE was determined to have a Pt utilization of 72%, which is substantially higher than that of the commercial ELAT electrode material (40%). This is reflected in Fig. 2(b), which shows CVs once they have been corrected for the Pt loading on the electrode. Furthermore, the ECSA of 67 $m^2\ g^{-1}$ achieved with the CCE is comparable to some of the largest ECSAs reported in the literature for E-Tek 20%Pt/Vulcan catalysts using Nafion-based ionomers [29,30] and substantially larger than those reported for the same electrocatalysts combined with SPEEK based ionomers [11,13,29].

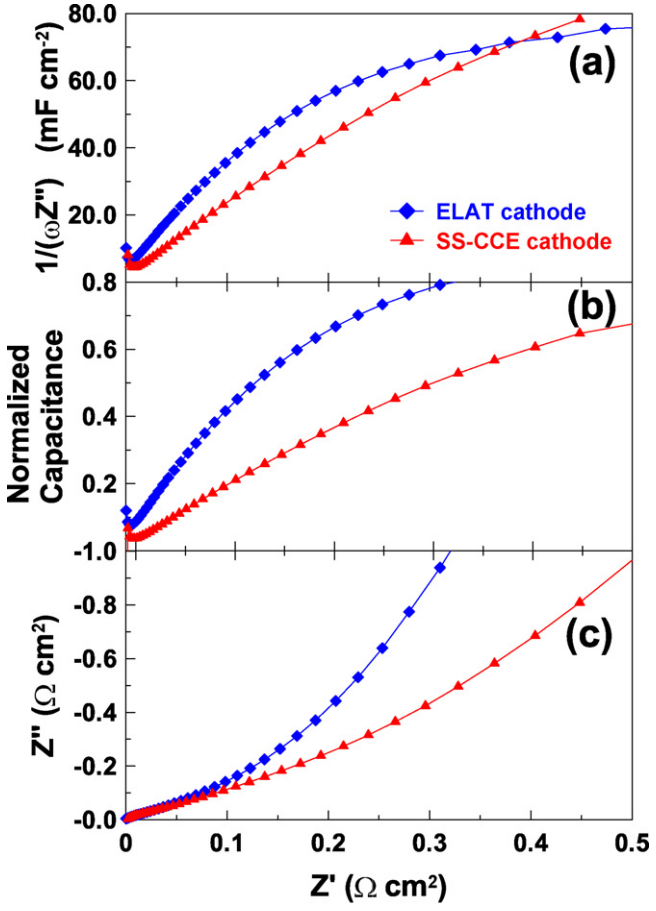

Fig. 4. Expansion of the high frequency region of Fig. 3.

Table 1
Comparison of the BET and electrochemical surface areas for different catalyst layers.

Cathode Composition	Pt loading (mg cm^{-2})	BET Surface Area (m^2 g^{-1})	Electrochemical Surface Area (m^2 g^{-1})	% Pt utilization (3 nm particles)
ELAT, prop. Nafion content	0.5	N A^{-1}	37	40
SS-CCE	0.34	382.2	67	72
TEOS CCE	0.21[a]	514.3	15[a]	16

[a] Data from Ref [22].

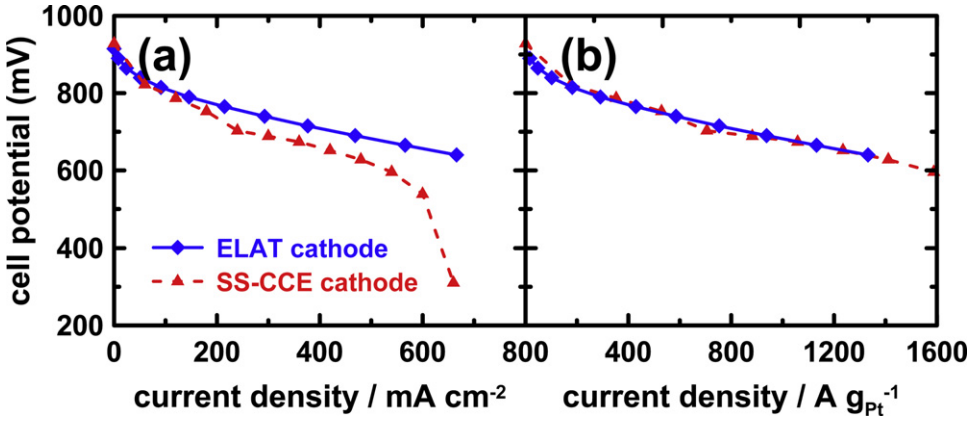

Fig. 5. Comparison of H_2/O_2 fuel cell polarization curves obtained for the SS-CCE cathode catalyst layers with that obtained with a Nafion-based ELAT cathode catalyst layer. Measurements were made at 80 °C at 100% RH with 10 psig backpressure on both sides.

The EIS spectra obtained for the SS-CCE and ELAT cathodes are shown in Fig. 3 as both capacitance plots (Fig. 3(a) and (b)) [31] and Nyquist plots (Fig. 3(c)). An expanded view of the high frequency region for each plot is shown in Fig. 4. Both the SS-CCE and the ELAT electrodes show steep slopes in the high frequency region of the capacitance plot, indicating similarly high proton conductivity for both the CCE and the Nafion-based catalyst layers [28,32]. Normalized capacitance plots, where the capacitance is normalized by dividing it by its limiting value, allow for comparison of proton conductivity of electrodes with different capacitive areas, are shown in Fig. 3(b). These highlight the similarly high proton conductivity of each electrode, though that within the ELAT electrode appears to be slightly higher.

Fig. 5 displays the fuel cell polarization curves obtained for both the SS-CCE cathode and the Nafion-based ELAT cathodes. Both MEAs give very similar performance, though the Nafion-based ELAT cathode performed slightly better at higher current densities. This can partially be attributed to the higher Pt loading in the ELAT electrode, as seen illustrated in Fig. 5(b). This performance difference may also be related to the hygroscopic nature of the SS-CCE that leads to mass transport limitations at high current densities. The CCE material readily retains water, making it more susceptible to flooding of the pores in the catalyst layer. However, this indicates that the SS-CCE may maintain performance under drier cathode conditions better than Nafion-based electrodes. Nonetheless, the performance of the CCE is remarkable given the complete absence of Nafion in the catalyst layer and is one of the highest performing non-Nafion based catalyst layers reported in the literature to date.

4. Conclusions

Sulfonated silane-based CCE were prepared by spray depositing the partially gelled CCE mixture. The resultant catalyst layers had very high ionic conductivity and consequently a high ECSA. Fuel cell tests show the SS-CCE material had similar fuel cell performance to that obtained with Nafion-based ELAT electrodes, indicating these SS-CCE are potential high performance Nafion-free alternative electrode structures for fuel cells.

Acknowledgements

This work was supported by the Natural Sciences and Engineering Research Council (NSERC) of Canada, and UOIT. We also thank Jeffery Powell (Trent University) for BET measurements. J.E. acknowledges NSERC and OGS for scholarship support.

References

[1] S. Litster, G. McLean, J. Power Sources 130 (2004) 61.
[2] E. Passalacqua, F. Lufrano, G. Squadrito, A. Patti, L. Giorgi, Electrochim. Acta 46 (2001) 799.
[3] E.B. Easton, Z.G. Qi, A. Kaufman, P.G. Pickup, Electrochem. Solid-State Lett. 4 (2001) A59–A61.
[4] A.W. Pedersen, A.D. Pauric, J.I. Eastcott, E.B. Easton, ECS Trans. 28 (27) (2010) 39.
[5] C.Y. Du, T.S. Zhao, Z.X. Liang, J. Power Sources 176 (2008) 9.
[6] Y.Y. Shao, J. Liu, Y. Wang, Y.H. Lin, J. Mater. Chem. 19 (2009) 46.
[7] Z.Q. Xu, Z.G. Qi, A. Kaufman, Electrochem. Solid-State Lett. 6 (2003) A171–A173.
[8] Z. Xu, Z. Qi, A. Kaufman, J. Power Sources 115 (2003) 49.
[9] Z.Q. Xu, Z.G. Qi, A. Kaufman, Electrochem. Solid-State Lett. 8 (2005) A313–A315.
[10] N. Lakshmi, N. Rajalakshmi, K.S. Dhathathreyan, J. Phys. D: Appl. Phys. 39 (2006) 2785.
[11] J. Peron, Z. Shi, S. Holdcroft, Energy Environ. Sci. 4 (2011) 1575.
[12] S. Sambandam, V. Ramani, J. Power Sources 170 (2007) 259.
[13] J. Peron, D. Edwards, A. Besson, Z.Q. Shi, S. Holdcroft, J. Electrochem. Soc. 157 (2010) B1230–B1236.
[14] J.S. Park, P. Krishnan, S.H. Park, G.G. Park, T.H. Yang, W.Y. Lee, C.S. Kim, J. Power Sources 178 (2008) 642.
[15] T. Astill, Z. Xie, Z. Shi, T. Navessin, S. Holdcroft, J. Electrochem. Soc. 156 (2009) B499–B508.
[16] E.B. Easton, T.D. Astill, S. Holdcroft, J. Electrochem. Soc. 152 (2005) A752–A758.
[17] J. Muldoon, J. Lin, R. Wycisk, N. Takeuchi, H. Hamaguchi, T. Saito, K. Hase, F.F. Stewart, P.N. Pintauro, Fuel Cells 9 (2009) 518.
[18] S. von Kraemer, M. Puchner, P. Jannasch, A. Lundblad, G. Lindbergh, J. Electrochem. Soc. 153 (2006) A2077–A2084.
[19] M. TSIONSKY, G. GUN, V. Glezer, O. LEV, Anal. Chem. 66 (1994) 1747.
[20] O. LEV, Z. Wu, S. Bharathi, V. Glezer, A. Modestov, J. Gun, L. Rabinovich, S. Sampath, Chem. Mater. 9 (1997) 2354.
[21] M.L. Anderson, R.M. Stroud, D.R. Rolison, Nano Lett. 2 (2002) 235.
[22] J.I. Eastcott, E.B. Easton, Electrochim. Acta 54 (2009) 3460.

[23] H. Kim, P.A. Kohl, J. Power Sources 195 (2010) 2224.
[24] Z.G. Qi, A. Kaufman, J. Power Sources 109 (2002) 38.
[25] S. Ranganathan, E.B. Easton, Int. J. Hydrogen Energy 35 (2010) 4871.
[26] N.E. De Almeida, E.B. Easton, ECS Trans. 28 (2010) 29.
[27] F. Maillard, M. Martin, F. Gloaguen, J.-M. Leger, Electrochim. Acta 47 (2002) 3431.
[28] E.B. Easton, P.G. Pickup, Electrochim. Acta 50 (2005) 2469.
[29] T. Astill, Z. XIE, Z.Q. Shi, T. Navessin, S. Holdcroft, J. Electrochem. Soc. 156 (2009) B499–B508.
[30] H.A. Gasteiger, S.S. Kocha, B. Sompalli, F.T. Wagner, Appl. Catal. B: Environ. 56 (2005) 9.
[31] X.M. Ren, P.G. Pickup, Electrochim. Acta 46 (2001) 4177.
[32] N.Y. Jia, R.B. Martin, Z.G. Qi, M.C. Lefebvre, P.G. Pickup, Electrochim. Acta 46 (2001) 2863.